Multifractal intermittency of Eulerian and Lagrangian turbulence of ocean temperature and plankton fields

L. Seuront[1], F. Schmitt[2*], D. Schertzer[2], Y. Lagadeuc[1] and S. Lovejoy[3]

[1]Station Marine de Wimereux, CNRS-URA 1363, Université des Sciences et Technologies de Lille, 28 avenue Foch, BP 80, 62930 Wimereux, France
[2]Laboratoire de Météorologie Dynamique, CNRS-UPR 1211, Université Pierre et Marie Curie, Tour 15, BP 99, 4 \place Jussieu, 75252 Paris Cedex 05, France
[3]Physics Dept., McGill University, 3600 University St., Montréal, H3A 2T8, Canada
*now at the Institut Royal Météorologique, Section Climatologie Dynamique, 3 avenue Circulaire, 1180 Bruxelles, Belgium

Abstract. In this paper, we present evidence that intermittency of Eulerian and Lagrangian turbulence of ocean temperature and plankton fields is multifractal and furthermore can be analysed with the help of universal multifractals. We analyse time series of temperature and *in vivo* fluorescence taken from a drifter in the mixed coastal waters of the eastern English Channel. Two analysis techniques are used to compute the fundamental universal multifractal parameters, which describe all the statistics of the turbulent fluctuations: the analysis of the scale invariant structure function exponent $\zeta(q)$ and the Double Trace Moment technique. At small scales, we do not detect any significant difference between the universal multifractal behavior of temperature and fluorescence in an Eulerian framework. This supports the hypothesis that the latter is passively advected with the flow as the former. On the one hand, we show that large scale measurements are Lagrangian and indeed we obtain for temperature fluctuations a ω^{-2} power spectrum corresponding to the theoretical scaling of a Lagrangian passive scalar. Furthermore, we show that Lagrangian temperature fluctuations are multiscaling and intermittent. On the other hand, the flatter slope at large scales of the fluorescence power spectrum points out that the plankton is at these scales a "biologically active" scalar.

1. Introduction

Scaling laws have been proposed in Eulerian (Kolmogorov, 1941a; Obukhov, 1941, 1949; Corrsin, 1951) and Lagrangian frameworks (Landau and Lifshitz, 1944; Inoue, 1950, 1951, 1952a, b; Lin, 1960; Monin and Yaglom, 1975) for velocity and passive scalar turbulence. In an Eulerian framework this general scaling picture has been confirmed with oceanic velocity (see e.g. Grant et al., 1962) and temperature data (Grant et al., 1968; Gargett et

al., 1984) over a wide range of scales. However, we are not aware of any reports of scaling spectra of oceanic turbulent measurements of either velocity or passive scalars taken in Lagrangian frameworks. In this paper, we perform both Eulerian and Lagrangian analyses of the intermittency of temperature fluctuations and fluorescence data (which is a proxy of phytoplankton biomass; see below). This comparison between Eulerian and Lagrangian frameworks appears to be of main interest to understand the effect of a sampling procedure on the characterization of a given process, but also to provide information about living organisms' perception of their fluid medium.

In vivo fluorescence measurements are used to test the hypothesis that living particles in turbulent fluid motions behave as passive scalars (Platt, 1972; Denman and Platt, 1976) whose Fourier spectral statistics are — to within intermittency corrections — known theoretically. This comparison allows us to study the nature of the couplings between the structure of phytoplankton populations and the structure of their physical environment (Legendre and Demers, 1984; Mackas et al., 1985). The statistics of fluorescence data have been previously analysed using power spectral analysis (Platt and Denman, 1975). However, the power spectrum is a second order moment, and is only sufficient for characterizing the variability if the latter is quasi-gaussian. On the contrary we find that the variability is far from gaussian — in accord with cascade theories — and give it a precise scale-by-scale and intensity-by-intensity characterization using multifractals. In contrast to the single exponent which is sufficient to characterize the scaling properties of fractal sets, the multifractal formalism generally describes scaling relations with an infinite family of scaling exponents (e.g. the fractal dimensions associated with different levels of fluid activity). However, due to the existence of stable, attractive, multifractal generators, only certain aspects of the multifractal dynamics will be important; we expect to

---

obtain universal multifractals (Schertzer and Lovejoy, 1987, 1989), in which this hierarchy is characterized by only three fundamental exponents.

Our multifractal characterization of biomass improves on the multifractal analysis of Pascual et al. (1995) in several ways. First, the use of universal multifractals makes the data analysis much more robust; only three fundamental parameters need to be estimated and we can use an analysis technique specially designed for their study (the Double Trace Moment technique, see Lavallée (1991) and Lavallée et al. (1992)). Second, using the notions of sampling dimensions and multifractal phase transitions, we can quantify the range of statistical moments which can be accurately estimated given the limited sample size. Other improvements with respect to Pascual et al. (1995) concern the pre-processing of the data which is performed in their paper, taking the square of the difference of fluorescence data. While this processing can be somewhat justified for velocity turbulence — at least if it can be measured at dissipation scales for plankton biomass —, it becomes here quite *ad hoc*. Is is certainly better first to directly analyse the data using structure functions, as we do here, and as is usually done in turbulence studies (see e.g. Monin and Yaglom, 1975). Finally, we also estimate the slopes of the power spectra of our data, which is essential in making comparisons with other fields and experiments.

In this paper, we present evidence that temperature and fluorescence variability can be characterized as universal multifractals. Since our data were taken from a drifting platform, they have the interesting properties that they exhibit both Eulerian and Lagrangian regimes. In section 2 we present the theoretical scaling relations for velocity and passive scalar turbulent fluctuations in Eulerian and Lagrangian framework, and in section 3 the data analysis.

2. Scaling relations for turbulent fields in Eulerian and Lagrangian frames

2.1 Eulerian relations for turbulent velocity and passive scalar fields

Scaling relations in Eulerian turbulence (Kolmogorov, 1941a; Obukhov, 1941, 1949; Corrsin, 1951) can be expressed using the energy flux ε and the scalar variance flux χ :

$$\varepsilon_l \approx \frac{(\Delta V_l)^3}{l} \tag{1}$$

$$\chi_l \approx \frac{(\Delta\theta_l)^2 \Delta V_l}{l} \tag{2}$$

where $\Delta V_i = |V(x+l) - V(x)|$ and $\Delta\theta_i = |\theta(x+l) - \theta(x)|$ are the velocity and temperature shears at scale l, $\Delta V_i / l$ is the inverse of the local eddy turnover time, and "$\approx$"

means equality of scaling laws, i.e. having the same scaling exponents (see below). Originally, these scaling relations where considered in the framework of homogeneous turbulence, i.e. the fluxes were considered as homogeneous, exhibiting no scale dependence. As a consequence, a unique exponent was required for the velocity and temperature, the famous 1/3 law in physical space, 5/3 for the energy or variance power spectra :

$$\Delta V_l \approx l^{1/3} \; ; \; E_V(k) \approx k^{-5/3} \tag{3}$$

$$\Delta\theta_l \approx l^{1/3} \; ; \; E_\theta(k) \approx k^{-5/3} \tag{4}$$

However, it is well known that this homogeneity assumption was theoretically and empirically untenable: fluxes are extremely inhomogeneous and scale dependent (therefore the subscript l in Eq. 1). But because the fluxes are conserved by the nonlinear terms of the equations of motion they are (on average) conserved during the cascade, i.e. their (ensemble) average should be strictly scale invariant :

$$\langle \varepsilon_l \rangle \approx \langle \varepsilon_1 \rangle \; ; \; \langle \chi_l \rangle \approx \langle \chi_1 \rangle \tag{5}$$

where the angle brackets "<.>" indicate statistical (ensemble) averaging. The corresponding (inhomogeneous) scaling relationship for the velocity field (Eq. 1) is often called the Kolmogorov refined similarity law (Kolmogorov 1962; Obukhov 1962) and the corresponding refining for the temperature fluctuations (Eq. 2) has been proposed for simulation and analysis of passive clouds (Schertzer and Lovejoy, 1987; Wilson et al., 1991; Pecknold et al.,1993).

In cascade models of turbulence, the highly inhomogenous fluxes are the results of a multiplicative process in which the variability is built up from large to small scales: larger structures are multiplicatively randomly modulated by smaller scales. In this case, this leads to multifractal fields, with the following multiscaling statistics (Schertzer and Lovejoy, 1987):

$$\langle (\varepsilon_l)^q \rangle \approx \lambda^{K_\varepsilon(q)} \tag{6}$$

$$\langle (\chi_l)^q \rangle \approx \lambda^{K_\chi(q)} \tag{7}$$

$$\langle [\Delta V_l]^q \rangle \approx \lambda^{-\zeta_V(q)} \tag{8}$$

$$\langle [(\Delta\theta_l)^2 \Delta V_l]^q \rangle \approx \lambda^{-\zeta_{V,\theta}(3q)} \tag{9}$$

with the relations, from Eqs. 1-2:

$$K_\varepsilon(q) = q - \zeta_V(3q) \; ; \; K_\chi(q) = q - \zeta_{V,\theta}(3q) \tag{10}$$

where L is a fixed outer scale and $\lambda = L/l$ is the corresponding scale ratio, $K_\varepsilon(q)$ and $K_\chi(q)$ are the scaling moment functions for the fluxes, $\zeta_V(q)$ is the scaling exponent of the (usual) velocity structure function and $\zeta_{V,\theta}(q)$ is the joint structure function scaling exponent of the product $(\Delta\theta_l)^2 \Delta V_l$. The strict scale invariance (Eq. 5) of the averaged fluxes yields $K_\varepsilon(1) = 0$

and $K_\chi(1) = 0$. Such multifractal fields are called "conservative multifractals". On the contrary, Eqs. 3-4 point out already that V and θ are not conserved. We may note that the conservation of the fluxes implies $\zeta_V(3) = 1$ and $\zeta_{V,\theta}(3) = 1$, which corresponds to the exact relations for the small-scale dissipation fields given by Kolmogorov (1941) and Yaglom (1949).

These relations (Eqs. 6-9), giving the scaling moment functions $K(q)$ and $\zeta(q)$, characterize all the fluctuations of the fluxes of energy and scalar variances and the fluctuations of the wind shears. But they do not directly give the scaling moment function $\zeta_\theta(q)$ of the passive scalar fluctuations, defined as:

$$\left\langle (\Delta\theta_l)^q \right\rangle \approx \lambda^{-\zeta_\theta(q)} \tag{11}$$

Indeed, the corresponding flux $\varphi_l = \varepsilon_l^{-1/2} \chi_l^{3/2}$ is a mixed flux of energy and scalar variance, which is non conservative. Obviously the two fluxes ε_l, χ_l are strongly correlated, so that the assumption of independence of the fluxes, used in Benzi et al. (1992), is a very simplistic hypothesis. An alternative is to relate this mixed flux to the structure function of the velocity and the temperature, as is done in Schmitt et al. (1996), which obtained the following expression, assuming statistical independence of the velocity and passive scalar fluctuations:

$$\zeta_\theta(q) = q/3 + K_s(q/6) - K_\chi(q/2)$$
$$\zeta_\theta(q) = \zeta_{V,\theta}(3q/2) - \zeta_V(q/2) \tag{12}$$

This expression was tested by Schmitt et al. (1996) on atmospheric turbulence data, with simultaneous records of wind velocity and temperature fluctuations. Unfortunately, since our Eulerian data gives only the passive scalar field without simultaneous velocity fluctuations, Eq. 12 cannot be tested here.

Nevertheless, we can analyze Eulerian scaling moment functions for a passive scalar using for $\zeta_\theta(q)$ the general expression for universal multifractals. Universal multifractals are the stable and attractive classes which are obtained with continuous multiplicative scaling processes (Schertzer and Lovejoy, 1987, 1989). In this framework the scaling moment functions $\zeta(q)$ (or $K(q)$[1]) have a precise theoretical shape:

$$\zeta(q) = Aq + Bq^\alpha \tag{13}$$

where A and B are constants and $0 \le \alpha \le 2$ is the Lévy index for stable variables (see e.g. Feller, 1971). This parameter is the most important, because, it describes the kind of multifractality of the field: for $\alpha = 0$, an inhomogeneous mono-fractal model is recovered (the β-model, see Frisch et al. (1978)), and for the other bound, $\alpha = 2$ corresponds to a lognormal multifractal (Kolmogorov, 1962; Obukhov, 1962; Yaglom, 1966). The condition of conservation of flux ($K(1) = 0$) yields an

expression which depends only on two parameters: C_1 is the codimension of the mean of the process, and verifies $0 \le C_1 \le 1$ (the larger is C_1, the more the field is inhomogeneous) and the Lévy index α:

$$K(q) = \frac{C_1}{\alpha - 1}\left(q^\alpha - q\right) \tag{14}$$

For the wind velocity field, the condition $\zeta_V(3) = 1$ and Eqs. 1, 13 give:

$$\zeta_V(q) = \frac{q}{3} - \frac{C_1}{\alpha - 1}\left(\left(\frac{q}{3}\right)^\alpha - \frac{q}{3}\right) \tag{15}$$

This equation has been used to characterize the wind velocity field in atmospheric turbulence (Schmitt et al., 1993, 1996; Schertzer et al., 1995), giving the values: $\alpha = 1.5 \pm 0.05$ and $C_1 = 0.15 \pm 0.03$.

For a scaling field which has no known condition of normalisation (as for example a passive scalar), we can write Eq. 13 on the following way:

$$\zeta_\theta(q) = qH - \frac{C_1}{\alpha - 1}\left(q^\alpha - q\right) \tag{16}$$

The new parameter H is there the degree of non-conservation of the average field ($\zeta_\theta(1) = H$): $H \ne 0$ means that the fluctuations are scale-dependent ($H \approx 0.38$ for temperature in atmospheric turbulence, see Schmitt et al. (1996)). The second term expresses a deviation from homogeneity (in which case $\zeta_\theta(q) = qH$), and represents the intermittency corrections. We use Eq. 16 to test the scaling behaviour of the temperature and fluorescence data, and determine these three parameters (H, C_1 and α).

2.2 Lagrangian relations for turbulent velocity and passive scalar fields

In a Lagrangian framework, as one follows the motion of an element of fluid, the scaling relations (Eqs. 1-2) are now to be expressed as a function of the difference of time (t) of observations (usually between actual time and initial time) instead of difference of location in an Eulerian framework. One obtain by replacing $\Delta V_l / l$ by $1/t$ in Eqs. 1-2 (Landau and Lifshitz, 1944; Inoue, 1950, 1951, 1952a, b; Lin, 1960; Monin and Yaglom, 1975):

$$\varepsilon_l \approx \frac{(\Delta V_l)^2}{t} \tag{17}$$

$$\chi_l \approx \frac{(\Delta\theta_l)^2}{t} \tag{18}$$

where $\Delta V_t = |V(\tau + t) - V(\tau)|$ and $\Delta\theta_t = |\theta(\tau + t) - \theta(\tau)|$ are the velocity and temperature fluctuations for an element of fluid on a time scale t (τ being the initial time). The assumption of a Lagrangian cascade for these fluxes (Novikov, 1989, 1990) leads *formally* to simpler scaling relations than in an Eulerian framework, since in

---

[1] For conservative processes, we use the notation $K(q)$.

Eq. 18 the scalar variance flux no longer depends *explicitely*[2] on a cross-product of velocity and temperature fields:

$$\left\langle \left(\varepsilon_t\right)^q \right\rangle \approx \Lambda^{K_\varepsilon(q)}; \quad \left\langle \left(\Delta V_t\right)^q \right\rangle \approx \Lambda^{-Z_V(q)} \tag{19}$$

$$\left\langle \left(\chi_t\right)^q \right\rangle \approx \Lambda^{K_\chi(q)}; \quad \left\langle \left(\Delta \theta_t\right)^q \right\rangle \approx \Lambda^{-Z_\theta(q)} \tag{20}$$

with the relations, given by Eqs. 17-18:

$$K_\varepsilon(q) = q - Z_V(2q); \quad K_\chi(q) = q - Z_\theta(2q) \tag{21}$$

where T is a fixed outer time-scale and $\Lambda = T/t$ is the corresponding time-scale ratio, $K_\varepsilon(q)$ and $K_\chi(q)$ are the Lagrangian scaling moment functions for the fluxes, $Z_V(q)$ is the Lagrangian velocity structure function scaling exponent and $Z_\theta(q)$ is the Lagrangian passive scalar structure function scaling exponent. The fluxes are still assumed to be conservative (i.e. their mean is scale-invariant): $K(1) = 0$. This implies $Z_V(2) = 1$ and $Z_\theta(2) = 1$.

Assuming universality (Eq. 14) for the (Lagrangian) flux of scalar variance, the (Lagrangian) structure functions' scaling exponents $Z_\theta(q)$ of a passive scalar depend only on the universal exponents (due to Eq. 21), whereas we pointed out that in the Eulerian framework the determination of the corresponding structure functions' scaling exponents is quite more involved and has not such a straightforward relationship with the scaling function of the variance flux. One may note that the transformations (for some other motivation) from space to space are somewhat discussed in Marsan et al. (1996).

2.3 Eulerian turbulent "biologically active" scalars

For chemically (Corrsin, 1961) or biologically (Denman and Platt (1976) and Denman et al. (1977)) active[3] scalars in turbulence, one usually assumes that there is a characteristic time, i.e. having a exponential decay (e.g. first order chemical reactions) or having an exponential population growth law. Due to this characteristic time, one expects a scalar variance spectrum with a slope -1 (as in the case of the Batchelor (1959) convective subrange, see below) for frequencies smaller than the corresponding characteristic frequency. The reason for this result is clear: for frequencies smaller than the characteristic frequency of the exponential law, the latter imposes its frequency, i.e. the flux of variance is no more ruled by turbulence, because it is too slow compared to the chemical reaction (here chlorophyll a synthesis) or population growth. Therefore, one must replace in Eq. 18 the inverse of the local eddy turnover time $1/t = \Delta V_l / l$ by this characteristic frequency ω_c, which gives:

$$\chi_{(F)l} \approx \left(\Delta F_l\right)^2 \omega_c \tag{22}$$

where F is the fluorescence concentration (which is a proxy of the phytoplankton concentration) and $\chi_{(F)}$ is the flux of scalar variance, as before. Then, the scalar variance being the Fourier transform of its spectrum, i.e.:

$$(\Delta F_l)^2 \approx E_F(k)k; \quad k \approx l^{-1} \tag{23}$$

we obtain, for the Fourier power spectrum of the biologically active scalar (Denman and Platt, 1976):

$$E_F(k) \approx \left(\Delta F_l\right)^2 k^{-1} \approx \chi_{(F)l}\omega_c^{-1}k^{-1} \tag{24}$$

As mentioned this spectrum is similar to Batchelor (1959) convective-subrange, although the mechanism is rather different. In case of convection it corresponds to high wave numbers (or frequencies), contrary to the case of the active scalar, where it occurs for lower frequencies. More precisely, the convective subrange is the range of the wave numbers where the molecular viscosity is already effective, whereas the molecular diffusion is not yet effective. This obviously requires a high Prandtl number (this number being the dimensionless ratio of the molecular viscosity and diffusivity). The convection results from non-local interactions, it is therefore the eddy turn at the beginning of the viscous subrange which will rule the convection.

Furthermore, fluorescence as a measure of phytoplankton abundance is a very special active scalar. For scales where the biological activities have time to develop (and is not destroyed by the turbulent motion), the phytoplankton cannot be considered as isolated: there are continuous predator-prey interactions, and two fluxes of creation and destruction of phytoplankton. Therefore, at large scales (when the biological time scales are of the same order as turbulent time scales), we still expect a highly intermittent phytoplankton density, but with characteristics clearly different from a passive scalar. In a previous paper (Seuront et al., 1996), we empirically analysed the biological activity and its multifractal characteristics in an Eulerian framework and confirmed this picture. We can here interprete these previous empirical results (Seuront et al., 1996) and propose, using Eq. 22, for the structure function scaling exponent $\zeta_F(q)$ of a biologically active scalar the following expression:

$$\zeta_F(q) = -K_\chi\left(\frac{q}{2}\right) \tag{25}$$

where $K_\chi(q)$ is the scaling exponent of the flux of fluorescence scalar variance. Because this flux is conservative ($K_\chi(1) = 0$), the biologically active scalar is not conservative: $\zeta_F(1) = -K_\chi(1/2) \neq 0$. We may notice that, up until now, there have been no attempts to study even the average fluctuations of the plankton variability in a Lagrangian frame, to our knowledge.

---

[2] Indeed the velocity was used to define implicitely the time.

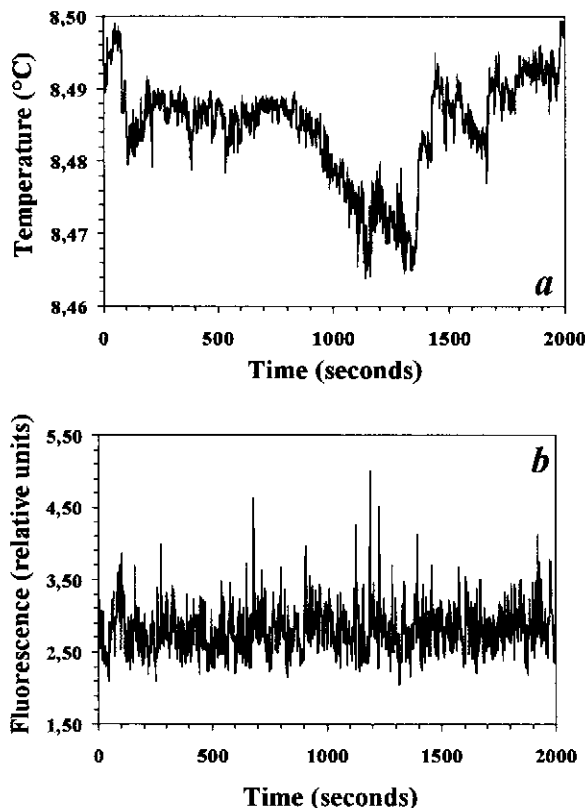[3] However, there are still dynamically passive, i.e. not influencing the velocity field.

Fig. 1. A portion of temperature (*a*) and *in vivo* fluorescence (*b*) time series recorded in the Southern Bight of the North Sea. Sharp fluctuations occuring on all time scales are clearly visible, indicating the intermittent behaviour of the dataset.

Fig. 2. The power spectrum of the turbulent fluorescence, shown in a log-log plot. The data are scaling from 0.04 to 1 Hz with a slope close to Kolmogorov power law trend of a passive scalar $E(f) \propto f^{-\beta}$ with $\beta \approx 1.66$. For lower frequencies, there is no evidence of a linear trend nor characteristic periods.

3. Empirical study of turbulent temperature and fluorescence

3.1 The data, their spectra and Eulerian/Lagrangian transition

The data were obtained as part as an experiment conducted adrift in tidally mixed coastal waters in the eastern English Channel, at the end of March 1995 during a period of spring tide. Temperature and *in vivo* fluorescence were simultaneously recorded during two hours at a 15m depth with a CTD recorder, (Sea Bird 25) and a fluorometer (Sea Tech), respectively. The sampling frequency ω being 2 Hz, our analysis are based on a time series of 11082 measurements, presented as a typical case of the variability of the different datasets sampled in this period. Samples of the data are shown in Fig. 1. One may note that the variability observed in the data used in our computation is always greater than the resolution of the measurements in both cases, and then is independent of any instrumental uncertainties.

We computed the Fourier power spectra of temperature and *in vivo* fluorescence fluctuations. The fluorescence power spectrum is shown in Fig. 2. It follows a power-law
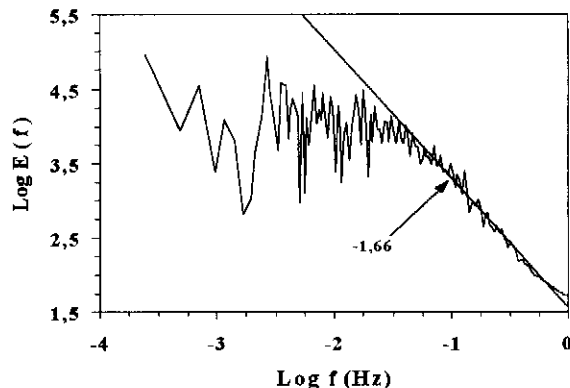
behaviour from 0.04 to 1 Hz according to:

$$E(\omega) \propto \omega^{-\beta} \tag{26}$$

where the slope β is close to the Obukhov-Corrsin Eulerian value 5/3 given by Eq. 4 (using the usual Taylor hypothesis to transform frequencies into a distance). In the multifractal frame, the intermittencies are taken into account noting that:

$$\beta = 1 + \zeta_\theta(2) \tag{27}$$

with $\zeta_\theta(2)$ given by Eq. 16, but empirically the correction to 5/3 is small for this second order of moment. For frequencies less than 0.04 Hz, fluorescence fluctuations do not exhibit evidence of power law behaviour nor characteristic periods. This is likely due to the shortness of the data set; it has been shown (Seuront et al., 1996) from a longer time series (but taken in an anchor station), that fluorescence data are scaling over smaller frequencies. This may also be due to the transition from Eulerian to Lagrangian sampling — see below.

The temperature power spectrum presents a mixed behaviour with two scaling tendencies for frequencies from 0.038 to 1 Hz ($\beta \approx 1.65$), and for frequencies lower than 0.038 Hz ($\beta \approx 2$) (Fig. 3a). These tendencies being difficult to distinguish, we transformed the spectral density by a multiplicative factor ω^2, and the resulting spectrum exhibits a power law behaviour with an exponent 0.35 ($r^2 = 0.95, p < 0.001$) which clearly breaks for frequency of about 0.038-0.040 Hz, lower frequencies being assimilated to a "noisy background" (horizontal tendency, see Fig. 3b).

In order to interpret this change in behaviour of the power spectrum, let us recall that the measurements are taken from a boat adrift in the Channel. For the high frequency range of the measurements we can consider the boat as not moving, so the measurements correspond to a
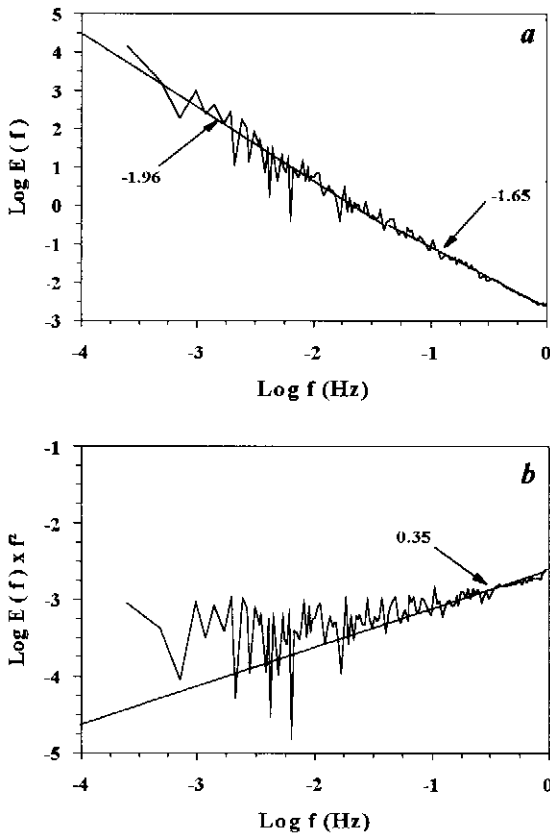
Fig. 3. The power spectrum of the turbulent temperature (a), shown in a log-log plot, exhibits a scaling behaviour for frequencies from 3.8 10^{-2} to 1 Hz with a spectral slope $\beta \approx 1.65$ and for frequencies greater than 3.8 10^{-2} Hz with a slope $\beta \approx 1.96$. The power spectrum, transformed by a factor ω^2 (b) confirms the scale breaking of the data, exhibiting a linear trend of 0.35 from 3.8 10^{-2} to 1 Hz.

Fig. 4. The temperature structure functions vs. $< |\Delta\theta_t|^q >$ vs. t in a log-log plot for $q = 1$, 1.5, 2 and 2.5 (from top to bottom), were $< |\Delta\theta_t|^q > = < (\Delta\theta_T)^q > (t/T)^{\zeta(q)}$. Linear trends are clearly visible for all order of moments, from 0.5 to 13s, for Eulerian scales (less than 13 seconds) and Lagrangian time scales (greater than 13 seconds). The straight lines indicate the best regression over each range of scales for each value of q. This gives in particular: $H = \zeta(1) = 0.34 \pm 0.01$ and $\zeta(2) = 0.65 \pm 0.02$ for Eulerian temperature and $H = \zeta(1) = 0.51 \pm 0.01$ and $\zeta(2) = 0.96 \pm 0.03$ for Lagrangian temperature.

fix-point procedure, i.e. Eulerian sampling. This is confirmed by the two small-scale spectra, each of them close to a -5/3 slope. The scale break exhibited by the temperature field for frequencies of about 0.038 Hz is associated with a characteristic time scale of 13 seconds. Using the instantaneous tidal circulation of about 1 m.s^{-1} observed during the field experiment, we estimate that the associated length scale is $\approx$ 13 meters, which is close to the size (12.5m) of the ship used during the sampling experiment (N/O Sepia II, CNRS-INSU). This means that for frequencies smaller than 0.038 Hz, the inertia of the boat becomes negligible and the measurements are effectively taken following the flows, i.e. in a Lagrangian framework. This transition is also confirmed by the spectral analysis of the temperature data which exhibit a spectral slope close to -2 as given by Eqs. 20-21 and 27. We may note here that contrary to the Eulerian frame where there are intermittency corrections to the spectral slope, in the Lagrangian frame we do not expect any intermittent correction for this second order moment (because here, the second order moment has the same scaling as a conserved flux: $\beta = 1 + Z_\theta(2) = 2 - K_\chi(1) = 2$.
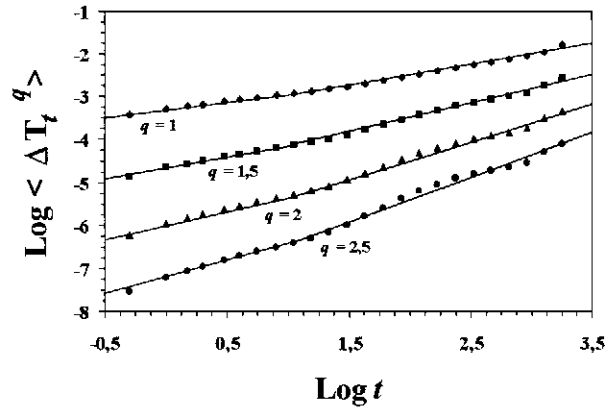
It is then possible to show that a time series recorded a priori in a oceanic Lagrangian framework can exhibit both Eulerian and Lagrangian components whose relative importance is determined by the size of the boat. We now determine the scale invariant properties of the intermittency of temperature and fluorescence fields, using direct multifractal analysis techniques.

3.2 Multifractal study of Eulerian intermittencies

We computed the structure functions $\langle (\Delta\theta_l)^q \rangle$ for the temperature field. Two power law regimes are visible in log-log plot (Fig. 4), consistent with the scale transition observed on the Fourier power spectrum. We obtain an Eulerian scaling over a range of scale from 0.5 s to 13 s (also observed for fluorescence field). We also estimated the structure functions for the fluorescence field.

In Fig. 5 we plotted the structure functions' scaling exponents $\zeta(q)$ obtained as the slopes of the straight lines for the range of scales 0.5 to 13 s. Here as below, the error bars come from the different portions of the dataset analysed separately: for example, with the scaling of Eulerian temperature and fluorescence up to 13 s and a database of 11082 points, we can estimate the exponents for 425 non-overlapping intervals. The scaling of the first exponents are very similar for temperature and fluorescence, respectively with $H = \zeta(1) = 0.34 \pm 0.02$ and $H = \zeta(1) = 0.36 \pm 0.02$, respectively. This is slightly smaller than the values obtained in Seuront et al. (1996) ($H = 0.42 \pm 0.02$ for temperature and 0.41 ± 0.02 for fluorescence), but nevertheless close to 1/3, the value corresponding to the Obukhov-Corrsin non-intermittent
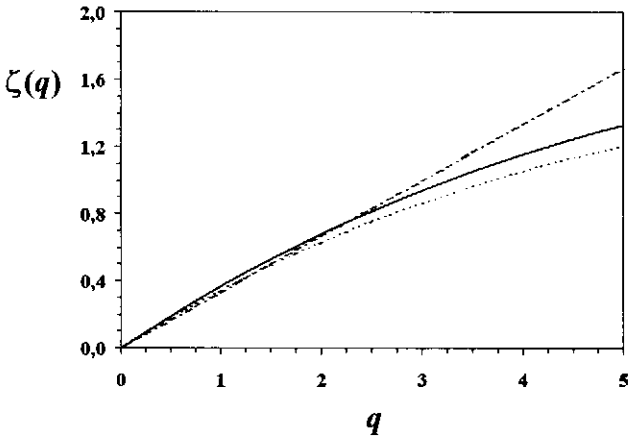
Fig. 5. Empirical values of $\zeta(q)$ obtained here for fluorescence (dashed line) and Eulerian (continuous line) temperature, compared to the homogeneous linear curve $\zeta(q) = q/3$ corresponding to Obukhov-Corrsin non-intermittent turbulence (discontinuous line). The nonlinearity of the empirical curves indicates multifractality.

passive-scalar turbulence. The scaling of the second order moments confirm the estimates from the power spectra ($\beta = 1 + \zeta(2)$), with $\zeta(2) = 0.66 \pm 0.02$ for fluorescence and $\zeta(2) = 0.65 \pm 0.02$ for temperature. More generally, for other orders of moments the non-linearity of the curves $\zeta(q)$ in Fig. 5 shows that these two fields can be considered as multifractals; the two curves corresponding to Eulerian sampling for temperature and fluorescence (i.e. phytoplankton biomass) are very close to each other. Within experimental error, they cannot be qualitatively considered as being different (we quantify is below). As shown in Seuront et al. (1996), this is a generalization of the result obtained by Denman and Platt (1976) who tested the assumption that the fluorescence was a passive scalar using only power spectra (a second order moment). Figure 5 shows that for all moments (and thus all intensities), fluorescence and temperature intermittencies have nearly the same probabilities. These multifractal statistics are compatible with the intermittent structure of the original time series (Fig. 1) which clearly exhibit numerous structures of different strengths and scales.

We now attempt to quantitatively characterize these intermittencies. Using Eq. (16) we have directly:

$$H = \zeta(1)$$
$$C_1 = H - \zeta'(1) \tag{28}$$

This gives $H \approx 0.34 \pm 0.02$, $C_1 \approx 0.037 \pm 0.004$ for temperature, and $H \approx 0.36 \pm 0.02$, $C_1 \approx 0.035 \pm 0.004$ for fluorescence. The value of α can be estimated using the best nonlinear fit of Eq. 16 (for $0 \leq q \leq 6.5$ and using a simple least-square method) of the empirical curve: we obtain for both temperature and fluorescence $\alpha \approx 1.8 \pm 0.05$. These values are quite close to those reported in Seuront et al. (1996): $H \approx 0.42$, $C_1 \approx 0.04$ and $\alpha \approx 1.7$ for temperature, and $H \approx 0.41$, $C_1 \approx 0.04$ and
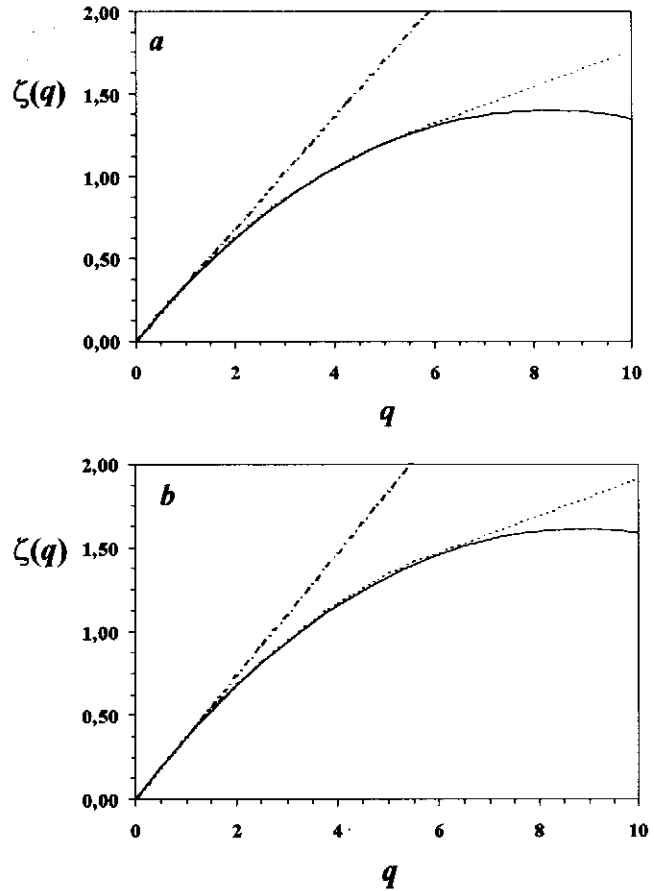

Fig. 6. The Eulerian scaling exponent structure function $\zeta(q)$ empirical curves (dashed line), compared to the homogeneous linear curve $\zeta(q) = q/3$ corresponding to Obukhov-Corrsin non-intermittent turbulence (discontinuous line), and to the universal multifractal functions obtain with H, C_1 and α in Eq. 16 (continuous line). The multifractal fit is excellent until moment order $q = 6.0 \pm 0.2$ for temperature (a) and $q = 6.2 \pm 0.2$ for fluorescence (b).

$\alpha \approx 1.8$ for fluorescence. The value of α we obtain shows that these fields are not lognormal multifractals ($\alpha = 2$), but also that the lognormal approximation for $\zeta(q)$ should not be too far from empirical estimates. The values of $C_1 \approx 0.04$ may seem to be quite small, but one must remember that this concerns the scalar field; if one considers the (non-conserved) flux (see Eq. 2):

$$\varphi_l = \varepsilon_l^{-1/2} \chi_l^{3/2} \approx \frac{(\Delta\theta)^3}{l} \tag{29}$$

then the value of C_1 must be transformed to $C_{1\varphi} = 3^\alpha C_{1\theta} \approx 0.27$. This values is larger than our latest estimate for the energy flux in the atmosphere (Schertzer et al., 1995; Schmitt et al., 1996): $C_1 \approx 0.15$; this shows that the scalar turbulence is more intermittent than the velocity turbulence.

Furthermore, within experimental error the values we obtain for temperature and fluorescence cannot be clearly

distinguished. We compared the empirical estimates with the theoretical curves in Fig. 6 (using Eq. 16 and the values above): the correspondence is excellent until moment order $q_T \approx 6.0 \pm 0.2$ and $q_P \approx 6.2 \pm 0.2$, after which the empirical curves are linear (Fig. 6). This linear behaviour of the empirical scaling exponent structure function $\zeta(q)$ is well-known for sufficiently high order moments (Schertzer and Lovejoy, 1989) and is due to sampling limitations (i.e. second order multifractal phase transition; see Schertzer and Lovejoy (1992)) or is associated with a divergence of statistical moments (i.e. first order multifractal phase transition; see Schertzer and Lovejoy (1992)) if substantiated by large enough sample size. Here with one realization of about 11,000 datapoints, the change in behaviour is likely to be due to sampling limitations. In this case, the critical moment q_s (for a scaling exponent structure function given by Eq. 16) is given by (Schertzer and Lovejoy, 1992):

$$q_s = \left(\frac{1}{C_1} \right)^{1/\alpha} \tag{30}$$

And in this case, the empirical $\zeta(q)$ follows:

$$\zeta(q) = 1 - \gamma_s q \quad ; \quad q \geq q_s \tag{31}$$

where γ_s is a maximum singularity associated to q_s. Here with the values estimated above, we obtain: $q_s \approx 6.2$ for temperature, and $q_s \approx 6.5$ for fluorescence, which are very close to the values previously proposed from the empirical curves. This critical moment is only linked to the sampling limitations; when more samples are taken into account in the statistics, it increases. In any case, most statistical parametrization basically dealing with maximum moment of order 3 (skewness), a critical moment greater than 6 then characterizes very rare events.

3.3 Multifractal study of Lagrangian intermittencies

As with Eulerian data above, we computed the structure functions for Lagrangian temperature which were shown to exhibit a scaling behaviour over scales greater than 13s. The corresponding behaviour of the fluorescence data is quite different, and it is not clear if there is some scaling or not (see Fig. 3); therefore, we do not proceed to the analysis of large-scales fluorescence field, leaving it to a future study. There is also an indetermination about the interpretation to give to this change of behaviour: is it due to Eulerian/Lagrangian transition, as for the temperature, or due to the biological activity, as obtained — for another dataset — in Seuront et al. (1996).

The scaling exponent for the first and second moments of the Lagrangian temperature are $Z_\theta(1) \approx 0.51 \pm 0.02$ and $Z_\theta(2) \approx 0.96 \pm 0.03$. The corresponding estimates for other moments gives the curve $Z_\theta(q)$, whose (slight) nonlinear behaviour (see especially the low order moments) is the signature of multifractal Lagrangian intermittency.
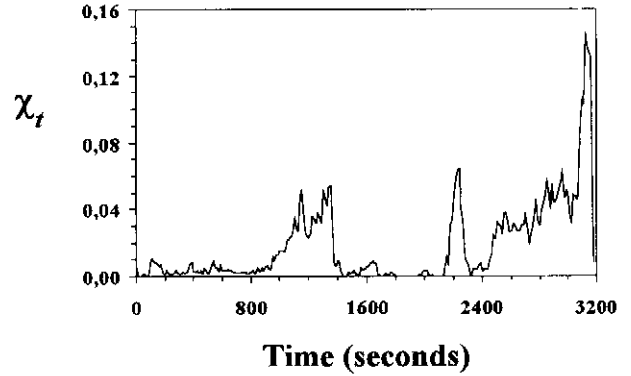

Fig. 7. Sample of the pattern of the rate of temperature variance transfert from large to small scales, showing intermittency.
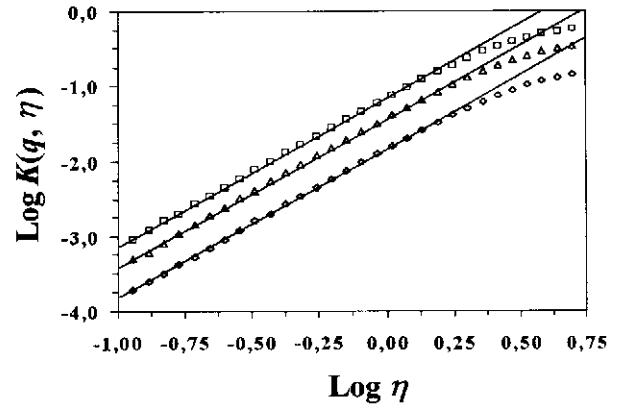

Fig. 8. The curves $K(q,\eta)$ vs. η in a log-log plot for $q = 2$, 2.5 and 3 (from bottom to top) for Lagrangian field χ_t, where $K(q,\eta) = \eta^\alpha K(q)$. The slopes of the straight lines then give the estimates of α: $\alpha \approx 1.8$ and C_1 is estimated by the intercept: $C_1 \approx 0.05$.

Let us recall here the simple expression for $Z_\theta(q)$, given by Eqs. 18, 20-21:

$$Z_\theta(q) = \frac{q}{2} - \frac{C_1}{\alpha - 1} \left(\left(\frac{q}{2} \right)^\alpha - \frac{q}{2} \right) \tag{32}$$

which directly gives the universal parameter C_1 as $C_1 = 1 - 2Z'(2)$. Here we obtain $C_1 \approx 0.05 \pm 0.01$. A simple way to estimate α is to take it as the best nonlinear fit of the data using Eq. 32. This gives $\alpha = 1.8 \pm 0.05$, the same value as what we obtain in the Eulerian case. We also verified these values by comparison with those obtained from the Double Trace Moment analysis (DTM) (Lavallée, 1991; Lavallée et al., 1992), which was applied on the data after a fractional differentiation of the temperature data of the order 1/2 (i.e. a $\omega^{1/2}$ multiplication in Fourier space, to remove the $t^{1/2}$ scaling of the first moment), and taking the square of the result, yielding an estimate of χ_t (see Eq. 18), whose pattern can be seen in Fig. 7.

The basic idea of the DTM technique is to generalize the application of statistical methods to the quantity
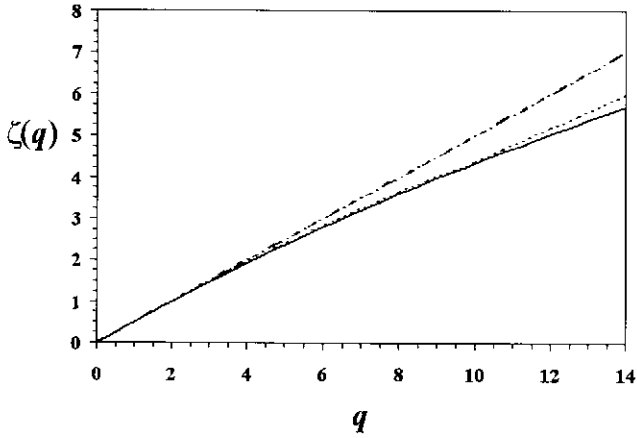
Fig. 9. The Lagrangian scaling exponent structure function $\zeta(q)$ empirical curves (dashed line) compared to the homogeneous Lagrangian turbulence linear curves $\zeta(q) = q/2$ (discontinuous line) and to the universal multifractal functions obtained with α and C_1 in Eq. 32 (continuous line). The universal multifractal fit is excellent until moment order $q \approx 10.4 \pm 0.5$ for temperature, corresponding to multifractal phase transition associated with sampling limitations.

$(\chi_\Lambda)^\eta$. This is done by taking the ηth power of χ_{Λ_0} at the scale ratio Λ_0 (the ratio of the outer or largest scale of interest to the smallest scale of homogeneity), and then studying its scaling behaviour at decreasing values of the scale ratio $\Lambda \le \Lambda_0$:

$$\chi_{\Lambda,\Lambda_0}(\eta) = \frac{(\chi_\Lambda)^\eta}{\langle (\chi_\Lambda)^\eta \rangle} \langle (\chi_{\Lambda_0})^\eta \rangle \tag{33}$$

The moments of this new field then have a multiple scaling behaviour, characterized by the new moment scaling function $K_0(q,\eta) = K(q\eta) - qK(\eta)$ (is a constant). For conservative universal multifractals, this gives, with the help of Eq. 14:

$$K_0(q,\eta) = \eta^\alpha K(q) \tag{34}$$

Then, by keeping q fixed (but different from the special values 0 or 1), the slope of $K_0(q,\eta)$ as a function of η on a log-log graph gives the values of the index α, which with the help of the intersection with the line ($\eta = 1$) yields C_1 (Fig. 8). This again gives $\alpha \approx 1.8$ and $C_1 \approx 0.05$, which confirms the values estimated above.

We then compare the universal multifractal fit obtained with α and C_1 in Eq. 32, with the empirical estimates. The universal multifractal and empirical fits were excellent until moment of about 10.4 ± 0.5, after which the empirical curves exhibit a linear behaviour (Fig. 9) which can reasonably be associated with sampling limitation because of the small number of data considered (because we had to average the original time series up to the scale of 13s, in order to be in the Lagrangian scales). This critical moment is given here by the following expression, obtained using Eq. 32, (it replaces Eq. 30, which was

Table 1. The values of the universal multifractal parameters obtained here, according to Eq. 16 for Eulerian values and Eq. 32 for Lagrangian (*a*), compared to the values we previously obtained in Seuront et al. (1996) (*b*). The values of the slopes of the Fourier power spectra are also indicated.

a	Eulerian data ($f > 0.038$ Hz) H, C_1 and α from Eq. 16				Lagrangian data ($f < 0.038$ Hz) C_1 and α from Eq. 32			
	β	H	C_1	α	β	H	C_1	α
Temperature	1.65	0.34	0.037	1.7	1.96	0.51	0.05	1.8
Fluorescence	1.66	0.36	0.035	1.8	-	-	-	-

b	Eulerian data passive scalar for $f > 0.01$ Hz				Eulerian data biologically active scalar for $f < 0.01$ Hz			
	β	H	C_1	α	β	H	C_1	α
Temperature	1.74	0.42	0.04	1.7	-	-	-	-
Fluorescence	1.75	0.41	0.04	1.8	1.22	0.12	0.02	0.8

obtained using Eq. 16):

$$q_s = 2\left(\frac{1}{C_1}\right)^{1/\alpha} \tag{35}$$

We obtain $q_s \approx 10.5$, which is very close to the empirical value given above.

4. Conclusion

It appears clearly from the present study that an *a priori* Lagrangian sampling may exhibit Eulerian and Lagrangian components separated by a length scale intimately linked to the size of the ship used to collect the field data. Indeed our results show that Eulerian and Lagrangian passive scalar turbulence exhibit multifractal statistics compatible with universal multifractals, in qualitative accord with the visual appearance of the time series. The values of the parameters are summarized in Tables 1a-b, which contain also the values reported in Seuront et al. (1996).

These analyses also provide an empirical confirmation of the ω^{-2} theory of the turbulent Lagrangian turbulent behaviour of a passive scalars. We obtained here a first evidence of Lagrangian multifractality, and we estimated the universal multifractal parameters (see also Table 1a-b), according to Eq. 32, which is a Lagrangian analogy of the refined similarity hypothesis for Eulerian turbulence. However, our Lagrangian study needed an averaging of the

dataset, which means that these results must be confirmed with much larger datasets, in order to be confident about the numerical values of the parameters.

On the other hand, *in vivo* fluorescence (a phytoplankton biomass proxy) appears to be a passive scalar on small scales (less than 13 seconds) associated with an Eulerian framework. Moreover, the commonality of the basic multifractal parameters of temperature and fluorescence reflects profound nonlinear couplings between the space-time structure of phytoplankton populations and the structure of their physical environment. As already noted in Seuront et al. (1996), this generalizes the results obtained in Denman and Platt (1976), with only a Fourier power spectrum analysis. In order to better understand the nature of the coupling between these fields, one direction for the future researches is to study their multifractal correlations; another is to analyze these fields in a vectorial multifractal framework.

Lastly, on larger scales (greater than 13 seconds) associated with a Lagrangian framework, the lack of scaling behaviour related to the small number of datapoints in the series does not allow us to explore the Lagrangian fluorescence variability, and to test Eq. 25: this will be done in future studies, using larger datasets.

References

Batchelor, G.K., Small-scale variation of convected quantities like temperature in turbulent fluid, Part I. General discussion and the case of small conductivity, *J. Fluid Mech.*, 5, 113, 1959.

Benzi, R., Biferale, L. and Parisi, G., Intermittency correction to the Obukhov-Corrsin theory of a passive scalar, *Europhys. Lett.*, 18, 213, 1992.

Corrsin, S., On the spectrum of isotropic temperature fluctuations in an isotropic turbulence, *J. Appl. Physics*, 22, 469-473, 1951.

Corrsin, S., The reactant concentration spectrum in turbulent mixing with a first-order reaction, *J. Fluid Mech.*, 11, 407-416, 1961.

Denman, K. L. and Platt, T., The variance spectrum of phytoplankton in a turbulent ocean, *J. Mar. Res.*, 34(3), 563-601, 1976.

Denman, K. L., Okubo, A. and Platt, T., The chlorophyll fluctuations spectrum in the sea, *Limnol. Oceanogr.*, 22, 1033-1038, 1977.

Feller, W., *An introduction to probability theory and its applications*, vol. II, second ed., John Wiley&Sons, New York, 1971.

Frisch, U., Sulem, P.-L., and Nelkin, M., A simple dynamical model of intermittent fully developed turbulence, *J. Fluid Mech.*, 87, 719, 1978.

Gargett, A. E., Osborn, T. R. and Nasmyth, P. W., Local isotropy and the decay of fluid turbulence in a stratified fluid, *J. Fluid Mech.*, 144, 231-280, 1984.

Grant, H., Stewart, R. and Moillet, A., Turbulent spectra from a tidal channel, *J. Fluid Mech.*, 12, 241-268, 1962.

Grant, H., Hugues, B., Vogel, W. and Moillet, A., The spectrum of temperature fluctuations in turbulent flow, *J. Fluid Mech.*, 34, 423-442, 1968.

Inoue, E., On the turbulent diffusion in the atmosphere, I, *Journal of the Meteorological Society of Japan*, 28, N°12, 441-456, 1950.

Inoue, E., On the turbulent diffusion in the atmosphere, II, *Journal of the Meteorological Society of Japan*, 29, N°7, 246-253, 1951.

Inoue, E., Turbulent fluctuations in temperature in the atmosphere and oceans, *Journal of the Meteorological Society of Japan*, 30, N°9, 289-295, 1952a.

Inoue, E., On the Lagrangian correlation coefficient for turbulent diffusion and its application to atmospheric diffusion phenomena, *Geophysical Res. Pap.*, N°19, 397-412, 1952b.

Kolmogorov, A. N., The local structure of turbulence in incompressible viscous fluid for very large Reynolds number, *Dokl. Acad. Nauk SSSR*, 30, 299-303, 1941a.

Kolmogorov, A. N., Energy dissipation in locally isotropic turbulence, *Dokl. Acad. Nauk SSSR*, 32, 19, 1941b.

Kolmogorov, A. N., A refinement of previous hypothesis concerning the local structure of turbulence in incompressible viscous fluid for very large Reynolds number, *J. Fluid Mech.*, 13, 82, 1962.

Landau, L. D. and Lifshitz, E. M., *Fluid mechanics*, Addison-Wesley, 1944 (first edition).

Lavallée, D., *Multifractal techniques: analysis and simulation of turbulent fields*, Ph.D. thesis, McGill University, Montréal, Canada, 1991.

Lavallée, D., Lovejoy, S. Schertzer, D. and Schmitt, F., On the determination of universal multifractal parameters in turbulence, in *Topological aspects of the dynamics of fluids and plasmas*, edited by K. Moffat, Tabor, M. and G. Zaslavsky, pp. 463-478, Kluwer, Boston, 1992.

Legendre, L. and Demers, S., Toward dynamic biological oceanography and limnology, *Can. J. Fish. Sci.*, 41, 2-49, 1984.

Lin, C., On a theory of dispersion by continuous movements, *Proc. Nat. Acad. Sci. USA*, 46, N°4, 556-570, 1960.

Mackas, D. L., Denman, K. L. and Abbot, M. R., Plankton patchiness: biology in the physical vernacular, *Bull. Mar. Sci.*, 37, 652-674, 1985.

Marsan, D., Schertzer, D. and Lovejoy, S., Causal space-time multifractal processes: predictability and forecast of rain fields, *J. Geophys. Res.* (in press), 1996.

Monin, A. S. and Yaglom, A. M., *Statistical Fluid Mechanics: Mechanics of turbulence*, MIT Press, London, 1975.

Novikov, E. A., Two-particle description of turbulence, Markov property, and intermittency, *Phys. Fluids A* 1, 326, 1989.

Novikov, E. A., The effects of intermittency on statistical characteristics of turbulence and scale similarity of breakdown coefficients, *Phys. Fluids A* 2, 814, 1990.

Obukhov, A., Spectral energy distribution in a turbulent flow, *Dokl. Akad. Nauk. SSSR*, 32, N°1, 22, 1941.

Obukhov, A., Structure of the temperature field in a turbulent flow, *Izv. Akad. Nauk SSSR Geogr. I Jeofiz.*, 13, 55-69, 1949.

Obukhov, A., Some specific features of atmospheric turbulence, *J. Geophys. Res.*, 67, 8, 3011, 1962.

Pascual, M., Ascioti, A. and Caswell, H., Intermittency in the plankton: a multifractal analysis of zooplankton biomass variability, *J. Plankton Res.*, *17*(6), 1209-1232, 1995.

Pecknold, S., Lovejoy, S., Schertzer, D., Hooge, C. and Malouin, J.-F., The simulation of universal multifractals, in *Cellular automata: prospects in astronomy and astrophysics*, eds. Perdang J.-M. and Lejeune A., World Scientific, 228, 1993.

Platt, T., Local phytoplankton abundance and turbulence, *Deep-Sea Res.*, *19*. 183-187, 1972.

Platt, T. and Denman, K. L., Spectral analysis in ecology, *Ann. Rev. Ecol. Syst.*, *6*, 189-210, 1975.

Schertzer, D. and Lovejoy, S., Physical modeling and analysis of rain and clouds by anisotropic scaling multiplicative processes. *J. Geophys. Res.*, *92*, 9693-9714, 1987.

Schertzer, D. and Lovejoy, S., Nonlinear variability in geophysics: multifractal analysis and simulation, in *Fractals: Physical Origin and Consequences*, edited by L. Pietronero, pp. 49-79, Plenum, New York, 1989.

Schertzer, D. and Lovejoy, S., Hard and soft multifractal processes, *Physica A*, *185*, 187-194, 1992.

Schertzer, D., Lovejoy, S. and Schmitt, F., Structures in turbulence and multifractal universality, in *Small scale structures in 3D hydro and MHD turbulence*, eds. M. Meneguzzi, A. Pouquet and P.L. Sulem, Springer, Lecture notes in physics vol. 462, 137, 1995.

Schmitt, F., Schertzer, D., Lovejoy, S. and Brunet, Y., Estimation of universal multifractal indices for atmospheric turbulent velocity fields, *Fractals*, 1, 3, 568, 1993.

Schmitt, F., Schertzer, D., Lovejoy, S. and Brunet, Y., Multifractal temperature and flux of temperature variance in fully developed turbulence, *Europhysics Letters*, 34, 3, 195, 1996.

Seuront, L., Schmitt, F., Lagadeuc, Y., Schertzer, D., Lovejoy, S. and Frontier, S., Multifractal analysis of phytoplankton biomass and temperature variability in the ocean, *Geophys. Res. Lett.* (in press), 1996.

Wilson, J., Lovejoy, S. and Schertzer, D., Physically based cloud modellling by multiplicative cascade processes, in *Nonlinear variability in geophysics: scaling and fractals*, eds. Schertzer D. and Lovejoy S., Kluwer Academic Press, Dordrecht-Boston, 185, 1991.

Yaglom, A. M., Local structure of the temperature field in a turbulent flow, *Dokl. Akad. Nauk SSSR*, *69*, 743, 1949.

Yaglom, A. M., The influence of fluctuations in energy dissipation on the shape of turbulent characteristics in the inertial interval, *Sov. Phys. Dokl.*, 2, 26, 1966.